Differential Cross Sections for the Ionization of Oriented H_2 Molecules by Electron Impact

J. Colgan,[1] M. S. Pindzola,[2] F. Robicheaux,[2] C. Kaiser,[3] A. J. Murray,[3] and D. H. Madison[4]
[1]*Theoretical Division, Los Alamos National Laboratory, Los Alamos, New Mexico 87545, USA*
[2]*Department of Physics, Auburn University, Auburn, Alabama 36849, USA*
[3]*School of Physics and Astronomy, University of Manchester, Manchester M13 9PL, United Kingdom*
[4]*Physics Department, Missouri University of Science and Technology, Rolla, Missouri 65409, USA*
(Received 15 September 2008; published 2 December 2008)

A nonperturbative close-coupling technique is used to calculate differential cross sections for the electron-impact ionization of H_2 at an energy of 35.4 eV. Our approach allows cross sections for any orientation of the molecule with respect to the incident electron beam to be analyzed. New features in the resulting cross sections are found compared with the case where the molecular orientation is averaged, and also with cross sections for He at equivalent electron kinematics. When averaged over all possible molecular orientations, good agreement is found with recent experimental results.

DOI: 10.1103/PhysRevLett.101.233201 PACS numbers: 34.80.Dp

Studies of the electron-impact ionization of small atoms and molecules continues to be the source of new discoveries as to the role of electron correlation in the break-up process, leading to new ways of investigating the electronic structure of the target. Measures of cross sections which are differential in both the energies and angles of the outgoing electrons [commonly known as triple differential cross sections (TDCS)] provide the most detailed information about the interaction between the outgoing electrons.

For simple atoms, good agreement now exists, for the most part, between experiment and several theoretical approaches for differential cross sections for the electron-impact ionization of H [1–4] and He [5–7]. For molecules, the problem is considerably more complex. The nonspherical nature of the target, along with the extra vibrational and rotational degrees of freedom inherent in even a simple diatomic molecule, make the theoretical description much more challenging. Consequently, most theoretical approaches to date have focused on ionization by high incident energy electrons where plane-wave impulse approximations may be employed, and where severe approximations, such as ignoring exchange effects [8], may be used. Another recent theoretical technique [9–11] which uses the three-body distorted-wave (3DW) approach (where distorted-waves are used to describe all incident and outgoing electrons) previously successfully used for atoms, also makes an orientation-average approximation, in which the molecular wave function used is averaged over all molecular orientations. This approach finds remarkably good agreement with experiment for most geometries considered ([11] and references therein).

One of the main motivations for studying ionization of diatomic molecules is the possibility of observing Young's slit type interference, as the ejected electron is scattered by the (two-center) diatomic molecule. This effect has been predicted theoretically [8] and subsequent experimental investigations [12] found indirect evidence of such an effect, although another study at lower energies found little effect [13]. Measurements to date only observe ionization from unoriented molecular targets, and so the ratio of the TDCS from H_2 and atomic H was proposed to more clearly elucidate such interference. A more recent study [14] found an oscillatory pattern in a similar ratio of H_2 to atomic He, which was claimed to be evidence for Young's type interference effects.

Most of these attempts to find signatures of Young's type interference in H_2 have focused on high incident energy electrons, since the wavelength is sufficiently short to be diffracted by the two-center ''slit'' provided by the two nuclei. Little attention (apart from a very recent study [11]) has been paid to scattering by low incident energy electrons from H_2. Theoretically, this can be a much more difficult problem, since the outgoing electrons are slow enough so that the interaction (including exchange) between them should be treated nonperturbatively. In this report we show, for the first time, how a nonperturbative close-coupling technique may be used to compute TDCS for electron-impact ionization of H_2 at an incident electron energy of 35.4 eV. We investigate the TDCS for equal energy shared between the outgoing electrons, which requires full treatment of the electron-electron interaction. A variety of geometries is considered; for most cases, excellent agreement is found between theory and measurement when we average over all possible molecular orientations. Furthermore we present, for the first time, TDCS from *oriented* molecules, so allowing subtle features in the angular distributions to be observed which are otherwise smeared out by the orientation averaging. To our knowledge, only one previous (experimental) study [15] has reported cross sections in which the molecular orientation is investigated, although the energy of the incident electrons in this case was very high and the final state of the ion was repulsive (leading to breakup of the molecule).

Our approach uses the time-dependent close-coupling (TDCC) technique [16], used previously to obtain total cross sections for electron-impact ionization of H_2^+ [17]

and H_2 [18]. Briefly, an expansion of the total electronic wave function in products of four-dimensional radial angular functions and rotational functions is used to express the Schrödinger equation in terms of a set of time-dependent coupled partial differential equations. The non-ionized electron of H_2 is frozen and its interaction with the two outgoing electrons is represented through direct and local exchange potential terms. The interaction between the two outgoing electrons is treated in full. The time-dependent equations are propagated for each M (projection of the angular momentum onto the z axis), l_0 (the incident angular momentum of the incident electron, represented by a Gaussian wave packet), and S (total spin angular momentum), for an incident electron energy of 35.4 eV and at the equilibrium internuclear separation of H_2. The TDCS can be expressed as

$$\frac{d^3\sigma}{dE_1 d\Omega_1 d\Omega_2} = \frac{\pi}{4k^2}\frac{1}{k_1 k_2}\sum_S (2S+1) \times \int dk_1 \int dk_2 \delta\left(\alpha - \tan^{-1}\frac{k_2}{k_1}\right)|\mathcal{M}|^2, \quad (1)$$

where k is the incident electron's momentum and k_1 and k_2 are the outgoing electron momenta (ejected into solid angles $\Omega_{1,2}$). For diatomic molecules, where the z axis is defined along the internuclear direction, and the incoming electron beam is oriented at angles (θ_k, ϕ_k) with respect to the z axis,

$$\mathcal{M} = \sum_{l_0}\sum_{M=-l_0}^{+l_0} i^{l_0} Y^*_{l_0 M}(\theta_k, \phi_k) \times \sum_{l_1,l_2}\sum_{m_1,m_2} (-i)^{l_1+l_2} e^{i(\sigma_{l_1}+\sigma_{l_2})} P^{l_0 MS}_{l_1 m_1 l_2 m_2}(k_1, k_2, T) \times Y_{l_1 m_1}(\hat{k}_1) Y_{l_2 m_2}(\hat{k}_2)\delta_{m_1+m_2,M}, \quad (2)$$

where $P^{l_0 MS}_{l_1 m_1 l_2 m_2}(k_1, k_2, T)$ is the wave function which results after projection of the four-dimensional radial and angular wave functions onto products of H_2^+ continuum states after propagation to a suitable time T. In Eq. (2), $Y_{lm}(\hat{k})$ is a spherical harmonic, and σ_l is the Coulomb phase shift. Our calculations were performed using a $384 \times 32 \times 384 \times 32$ lattice for the $(r_1, \theta_1, r_2, \theta_2)$ spherical polar coordinates, with a uniform mesh spacing of $\Delta r = 0.2$ a.u. and $\Delta\theta = 0.031\,25\pi$, for all l_0, M values from 0 to 6, and for $S = 0, 1$. The wave functions for $-M$ values were assumed equal to those for $+M$ values, which was confirmed by several explicit calculations for selected $-M$ values.

In Fig. 1 we compare our TDCC calculations with measurements made using the experimental apparatus described previously [5,13]. The experiments were performed for various values of ψ, which is the angle between the incident electron gun angle and the plane in which the two outgoing electrons are detected. The outgoing electrons are measured in coincidence where 2ξ is

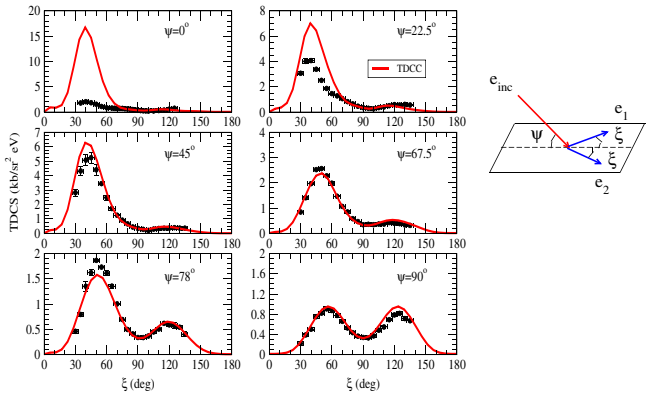

FIG. 1 (color online). TDCS for the electron-impact ionization of H_2, for various configurations of the experimental gun angle ψ. TDCC calculations (red lines), where the calculations have been averaged over all molecular orientations, are compared with the measurements.

the mutual electron angle. $\psi = 0°$ represents a coplanar geometry and $\psi = 90°$ is known as the perpendicular geometry. In the measurements the molecular orientation is unknown, and so the TDCS is computed for all possible (θ_N, ϕ_N) (these are the angles the molecule makes with the z axis in the Lab frame, where in the Lab frame the z axis is defined by the electron beam direction), which are then averaged to compare with the measurements. A common point which exists at $\xi = 90°$ for any value of ψ (confirmed in the calculations) allows the experimental results to be relatively normalized. In Fig. 1 the experiment has been normalized to the absolute TDCC calculations for the $\psi = 90°$ case. For large values of ψ the averaged TDCC calculations are in excellent agreement with experiment, for both the shape and (relative) magnitude of the TDCS. The TDCC calculations describe the binary and recoil peaks very well. At lower values of ψ, and especially for $\psi = 0°$, the shape of the calculations matches the measurements quite well, but theory and experiment differ considerably as to the magnitude of the dominant binary peak. It is at present unclear as to the source of this discrepancy. All the cross sections presented in Fig. 1 are obtained from a single set of TDCC calculations, which should have the same convergence properties. It seems unlikely then that the disagreement in Fig. 1 for the comparison for $\psi = 0°$ can be ascribed to a lack of convergence in the TDCC calculations. It is also interesting that the measurements predict that the largest cross sections are found for an incident gun angle of 45°, unlike the TDCC calculations which predict that the largest cross sections are for the coplanar case. In similar He studies, both theory and experiment find that the largest cross sections are also found for the coplanar case. Clearly, further studies are required to resolve this discrepancy.

In the remaining figures we examine more closely two of the geometries considered in Fig. 1, the perpendicular ($\psi = 90°$) and coplanar ($\psi = 0°$) cases. Here we also present TDCC calculations for three cases where the mo-

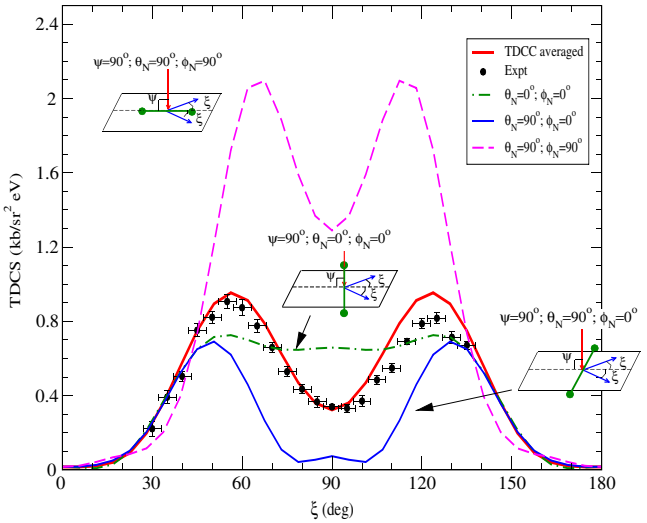

FIG. 2 (color online). TDCS for $\psi = 90°$. TDCC calculations averaged over all molecular orientations (red line) are compared with experiment. The green dot-dashed, blue solid, and magenta dashed lines represent TDCC calculations for various orientations of the molecule with respect to the beam direction, as indicated.

lecular orientation (with respect to the Lab frame z axis defined by the incoming electron beam) is fixed. In Fig. 2, the perpendicular case, substantial differences are found for the oriented TDCS compared with the averaged case. When the molecule lies along the incident beam direction (dot-dashed green line) the resulting TDCS is almost flat in the middle of the distribution, unlike the averaged case, which shows a pronounced dip. However when the molecule is perpendicular to the incident beam direction and the axis between the two detected electrons ($\theta_N = 90°$, $\phi_N = 0°$, blue line), the dip in the TDCS is even more pronounced than the averaged case, and in fact the cross section is almost zero for $\xi = 90°$. Clearly the positioning of the molecule further inhibits electron ejection at $\xi = 90°$, since the ejected electrons will be repelled by the $1s\sigma_g$ charge cloud of the remaining H_2^+ electron, which will predominantly lie along the molecular axis. When the molecule is oriented perpendicular to the incoming beam direction (dashed magenta line) and lies along the axis between the outgoing electrons, the TDCS has a similar shape to the averaged case, but has a much greater magnitude. In this case the molecular position has less effect on the electron angular distribution, since there is very low probability of electron ejection at $\xi = 0°$, due to electron repulsion. When the molecule lies along the beam direction, no dip is seen at $\xi = 90°$ because the ejected electrons are in a plane perpendicular to the nuclei and $1s\sigma_g$ charge cloud, and so largely unaffected by the molecule. We also note that the shape of any of these TDCS is quite different from the corresponding TDCS for He, for the same excess energy conditions. For He, the measurements for this geometry show a strong peak in the TDCS at $\xi = 90°$ [19], which is confirmed by CCC [6] and TDCC calculations.

It is interesting to study how the TDCS varies as the molecule moves between the orientations described in Fig. 2. For example, we can examine the change in the TDCS as the molecule moves from the case where it is aligned along the incoming beam axis ($\theta_N = \phi_N = 0°$) towards the $\theta_N = \phi_N = 90°$ case (dashed magenta line in Fig. 2) or towards the $\theta_N = 90°$; $\phi_N = 0°$ case (solid blue line in Fig. 2). The TDCS for various intermediate θ_N values are shown in Fig. 3, for $\phi_N = 90°$ (upper panels) and $\phi_N = 0°$ (lower panels). In the $\phi_N = 90°$ case, the TDCS remains symmetric around $\xi = 90°$ as θ_N is varied. However, for $\phi_N = 0°$, the TDCS loses its symmetry around $\xi = 90°$ at θ_N values between 0° and 90°. This surprising result highlights the interesting physics inherent in examining TDCS for particular molecular orientations. The symmetric TDCS found when averaging over all

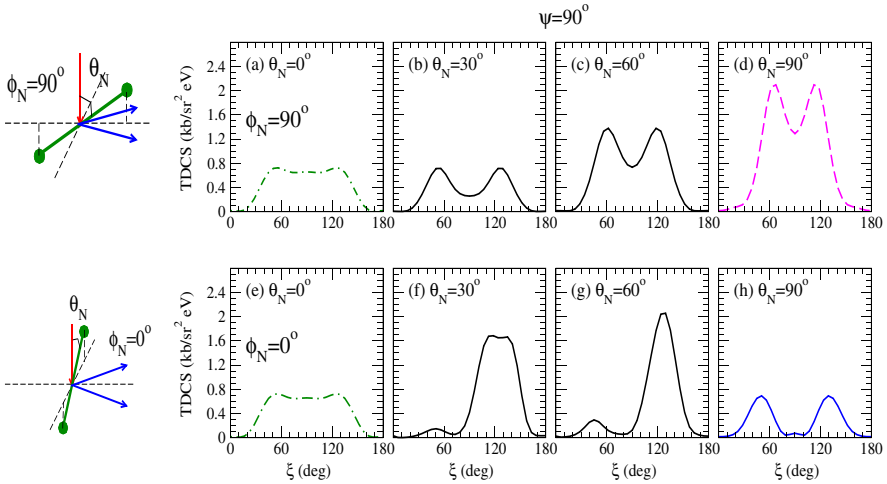

FIG. 3 (color online). TDCS for various fixed values of (θ_N, ϕ_N), the angles between the molecule and the incoming electron beam, when $\psi = 90°$. The upper panels are for $\phi_N = 90°$ and the lower panels for $\phi_N = 0°$.

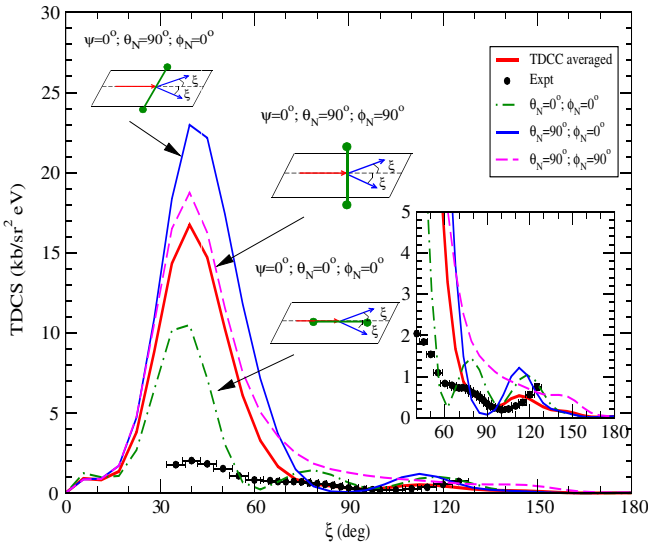

FIG. 4 (color online). As in Fig. 2, for the case where $\psi = 0°$.

molecular orientations can still be understood because the unsymmetric TDCS found for the molecular angles in Fig. 3 are compensated by TDCS for $90° < \theta_N < 180°$ which are mirror images of the lower panels in Fig. 3. The reason for the unsymmetric TDCS in the lower panels of Fig. 3 can be difficult to pin down, since the TDCS is influenced strongly not only by the position of the molecule with respect to the outgoing electrons, but also by the interactions between the outgoing electrons. The asymmetry may be due to greater scattering from the nuclei by the incoming electron for intermediate θ_N values. Since the target is not spherically symmetric in these cases, the TDCS loses its symmetry. For $\theta_N = 0°$ and $\theta_N = 90°$, the incoming beam does see a spherically symmetric target, resulting in a symmetric TDCS. In the upper panels (when $\phi_N = 90°$), the TDCS may remain symmetric since the molecule is still confined to the plane between the outgoing electrons.

For the coplanar ($\psi = 0°$) case presented in Fig. 4, less dramatic differences are observed when the molecular orientation is fixed. The binary peak dominates for all orientations, as also found in the averaged case. However, we do find that, in the case where the molecule is aligned along the beam direction (dot-dashed green line), an extra peak is found at $\xi \sim 80°$ between the binary and recoil peaks (as shown in the inset). This extra peak is not observed in the calculations averaged over all orientations, although there is a hint of an extra peak in the experimental data at this angle. This extra peak may be due to the importance of higher partial wave contributions in this case, since for ionization, larger partial wave components of the initial wave packet are required to overcome the positioning of the nuclei. We also note that, for the case where the molecule is aligned perpendicular to the incoming beam and perpendicular to the plane in which the electron are detected (dashed magenta line), no secondary peaks appear to be present. This may be due to the fact that the molecule is out of the plane containing all the electrons, and so the molecular position is less important, also inhibiting a recoil peak usually caused by nuclear scattering of one of the ejected electrons.

We also wish to emphasize that the extra structures observed in the TDCS shown here for H_2, both for calculations where the TDCS is averaged over all orientations, and for fixed molecular orientations, should not be attributed to some type of Young's slit two-center interference. The kinematics considered here are such that both outgoing electrons have 10 eV, which corresponds to an electron wavelength much longer than the internuclear H_2 separation of 1.4 a.u. Therefore no Young's slit interference should be expected. Rather, the differences between the TDCS observed for H_2 and He should be attributed to the different structure of the bound electrons in each system, and also to the different Coulombic potentials in which the outgoing electrons move in each case. These findings also raise the possibility that the extra features in the TDCS observed at high incident energies [12,14] are not necessarily due to Young's slit interference, but may be due simply to the different electronic structure of the molecular target.

A portion of this work was performed under the auspices of the US DOE through Los Alamos National Laboratory (LANL) and through DOE and NSF grants to Auburn University. Computational work was carried out at the NCCS in Oak Ridge, TN, and through a LANL Institutional Computing Resources grant. A portion of this work was done under National Science Foundation grant No. PHY-0757749, and we acknowledge the EPSRC (UK) for support of the experimental work.

[1] J. Röder *et al.*, Phys. Rev. Lett. **79**, 1666 (1997).
[2] T. N. Rescigno *et al.*, Science **286**, 2474 (1999).
[3] I. Bray, Phys. Rev. Lett. **89**, 273201 (2002).
[4] J. Colgan *et al.*, Phys. Rev. A **74**, 012713 (2006).
[5] A. J. Murray and F. H. Read, J. Phys. B **26**, L359 (1993).
[6] A. T. Stelbovics *et al.*, Phys. Rev. A **71**, 052716 (2005).
[7] J. Colgan *et al.*, Phys. Rev. A **73**, 042710 (2006).
[8] C. R. Stia *et al.*, J. Phys. B **36**, L257 (2003).
[9] J. Gao *et al.*, Phys. Rev. A **72**, 020701(R) (2005).
[10] J. Gao *et al.*, J. Phys. B **39**, 1275 (2006).
[11] O. Al-Hagan *et al.*, Nature Phys. (to be published).
[12] D. S. Milne-Brownlie *et al.*, Phys. Rev. Lett. **96**, 233201 (2006).
[13] A. J. Murray, J. Phys. B **38**, 1999 (2005).
[14] E. M. Staicu-Casagrande *et al.*, J. Phys. B **41**, 025204 (2008).
[15] M. Takahashi *et al.*, Phys. Rev. Lett. **94**, 213202 (2005).
[16] M. S. Pindzola *et al.*, J. Phys. B **40**, R39 (2007).
[17] M. S. Pindzola *et al.*, J. Phys. B **38**, L285 (2005).
[18] M. S. Pindzola *et al.*, Phys. Rev. A **73**, 052706 (2006).
[19] A. J. Murray *et al.*, J. Phys. B **25**, 3021 (1992).